2.N Nuclear Physics A331 (1979) 213–236; © North-Holland Publishing Co., Amsterdam

A MICROSCOPIC DESCRIPTION OF NUCLEAR MOLECULES: Application to the $^{12}C+^{12}C$ system

J. CUGNON †, H. DOUBRE and H. FLOCARD ††

Divisions de Physique Nucléaire et Théorique, Institut de Physique Nucléaire, 91406 Orsay Cedex, France †††

Received 24 January 1979
(Revised 15 May 1979)

Abstract: The interaction energy between two oblate ^{12}C ions is calculated by means of the constrained Hartree-Fock method. The influence of the mutual orientation of the ions is investigated by considering two extreme configurations: an axial symmetric one where the two ions approach each with their symmetry axes aligned with the collision axis and a triaxial one where the axes of the fragments are perpendicular to the collision line. The corresponding potentials V_1 and V_2 display very distinct features. In particular the minima of the potentials occur for quite different interdistances. A method is devised for constructing from V_1 and V_2 the potentials and coupling factors between two ions rotating with definite angular momentum. Using these quantities in a coupled channel calculation, we explain the gross features of the elastic, single 2^+ inelastic and double inelastic cross sections. The same calculation yields good agreement with the fusion data.

1. Introduction

The discovery of correlated structures [1]) in several reaction yields of the $^{12}C+^{12}C$ system has been the starting point of a systematic experimental investigation. Its results can be summarized as follows. For energies close to that of the Coulomb barrier, 500 keV wide correlated structures have been observed. At higher energies the elastic excitation functions display a gross structure with 2 to 4 MeV wide bumps [2, 3]). In addition, a number of fine structures have been observed in the elastic and numerous reaction cross sections (for a review, see ref. [4])). The fine structure (few keV wide) is likely to have a statistical origin, while most of the intermediate structure (500 keV wide) and the whole gross structure are thought to be connected with entrance channel phenomena. Detailed studies of the excitation functions for inelastic channels (in which one or both ^{12}C nuclei are excited to the first 2^+ state) are also available [5, 6]). Their main and surprising result is that the inelastic yields are of the same order of magnitude as the elastic cross section over a wide range of bombarding energies. Moreover, some angle-integrated cross-section measurements have also been performed [6–8]). However, the results somewhat disagree from one experiment to the other, although the presence of wide bumps seems now rather

† Permanent address: Institut de Physique, Université de Liège Sart-Tilman B-4000 Liège 1, Belgique.
†† Present address: Nuclear Science Division L.B.L. Berkeley California 94720 USA.
††† Laboratoire associé au CNRS.

well established. Finally, the fusion cross section measured up to 30 MeV (c.m.) displays an oscillatory structure with a period of several MeV [ref. [9])].

The theoretical effort has paralleled the experimental achievements. The emphasis has first been put on explaining the narrow structures for bombarding energies close to that of the Coulomb barrier. More recently, various models have been proposed which attempt an explanation of a larger body of data. One may distinguish three main types of approaches:

(i) A theory based on the α-cluster picture [10]) assigns the gross structure of the elastic scattering to quasibound states in a potential describing the interaction between two unperturbed carbons, and the fine structure to metastable states of a system composed of a carbon core and three α-particles. The decay of these states feeds the compound nuclear system. The theory has however remained mainly at a qualitative level despite some success in explaining the branching ratios for the α-particle channels.

(ii) In a group of phenomenological or semimicroscopic models [11-17]), the inelastic channels corresponding to the excitation of the first 2^+ state of one or both of the two carbons are included explicitly. The gross structure in the elastic cross section is still associated unbound eigenstates in the elastic potential well. These resonances are usually broad since they occur near or above the interaction barrier. Furthermore they are coupled to quasibound states in the inelastic potential wells. These states have generally a much smaller width because they lie deeper in the potential well. This pattern of broad and narrow interacting resonances has received names like double resonances [15]) or band crossing [14]). In most of these works, only the potential (escape) width of the quasibound states is considered. When cross sections are calculated, the spreading width due to the coupling with the compound nuclear states is introduced by means of an absorptive potential. However, in order not to wash out the fine structure, the magnitude of the absorptive potential is always kept very small despite what is suggested by the large fusion cross section [9]).

(iii) In a third kind of approach [18]), one attempts a simultaneous explanation of the fine structure, and of the magnitude of the absorption. The latter is obtained by the introduction of a conventional absorptive potential, while fine structure is due to a resonant Landau-Zener coupling of the elastic potential curves with "anomalous" potential curves associated with excited configurations and crossing each other outside the range of the absorption. However, the theoretical justification of the anomalous potential is still an open problem.

The approacn followed in this paper is in the line of the second group cited above. However we insist on keeping phenomenology at the lowest possible level. With the Skryme interaction SIII, we compute, the Hartree-Fock (HF) interaction between two ^{12}C nuclei as a function of their relative distance. The use of an effective nucleon-nucleon interaction successfully tested on a large body of very different nuclear properties [19]) is an important feature of our calculation. This contrasts with most of the ^{12}C-^{12}C potentials used in the references above, which are either derived

phenomenologically [11-16]) or by means of *ad hoc* nucleon-nucleon interactions [17]). The deformation of the intrinsic state of ^{12}C leads to consider the potentials corresponding to different orientations of the ^{12}C nuclei with respect to the line joining their centres of mass. From them a method is proposed to construct the potentials and the coupling terms of the system of coupled equations describing the single and mutual excitation to the 4.43 MeV 2^+ state of ^{12}C. We also discuss the connection of our approach with the Born-Oppenheimer method and molecular nuclear physics. Finally we show the predictions of our model concerning several cross sections including the fusion cross section.

2. Potential energy curves

In this section we investigate the influence of the mutual orientation of the two deformed ^{12}C nuclei on their interaction energy. This quantity is obtained by Hartree-Fock calculations in which the total mass quadrupole moment is constrained.

We use the Skyrme nucleon-nucleon effective interaction SIII [ref. [20])]. The direct part of the Coulomb force is also included. Since we assume a perfect spin up-spin down degeneracy the spin-orbit part of the Skyrme force has been neglected. The HF equations are solved in configuration space by means of a triaxial code. The single particle wave functions are discretized on a three-dimensional mesh. The mesh size has been chosen so as to ensure a 100 keV accuracy of the results. Details on the numerical procedure may be found in ref. [21]). In addition to the spin degeneracy, spatial symmetries are assumed for the total ^{12}C+^{12}C system. Let us call O the position of the total center of mass and Ox the collision axis. We impose the parities with respect to the $x = 0$, $y = 0$, and $z = 0$ planes to be good quantum numbers for the single particle wave functions. No correction for the center-of-mass motion has been applied. This is consistent with the adiabatic time dependent Hartree-Fock (ATDHF) method [22]). In this method the collective potential is defined, like here, as the constrained HF energy (CHF) and a possible center-of-mass effect as well as other effects of more dynamical origin are taken into account by the replacement of the reduced mass by an effective mass. Calculation of this effective mass is presently underway [23]).

With the nucleon-nucleon interaction used in this work the ground state of ^{12}C is oblate with a quadrupole moment $Q_f = -39$ fm^2. It therefore exists a triple continuous set of possible mutual orientations of the two ^{12}C nuclei. We have investigated two extreme cases which are depicted by diagrams 1 and 2 of fig. 1. The first configuration is axially symmetric. The two ions approach each other with their symmetry axis aligned with the direction of the collision. The second case leads to a triaxial shape with the two ^{12}C axes perpendicular to the collision axis.

To obtain a given orientation of the fragments we impose the proper asymptotic parities of the wave functions with respect to the three symmetry planes and keep these parities as the two ^{12}C nuclei approach each other and interact. The potential

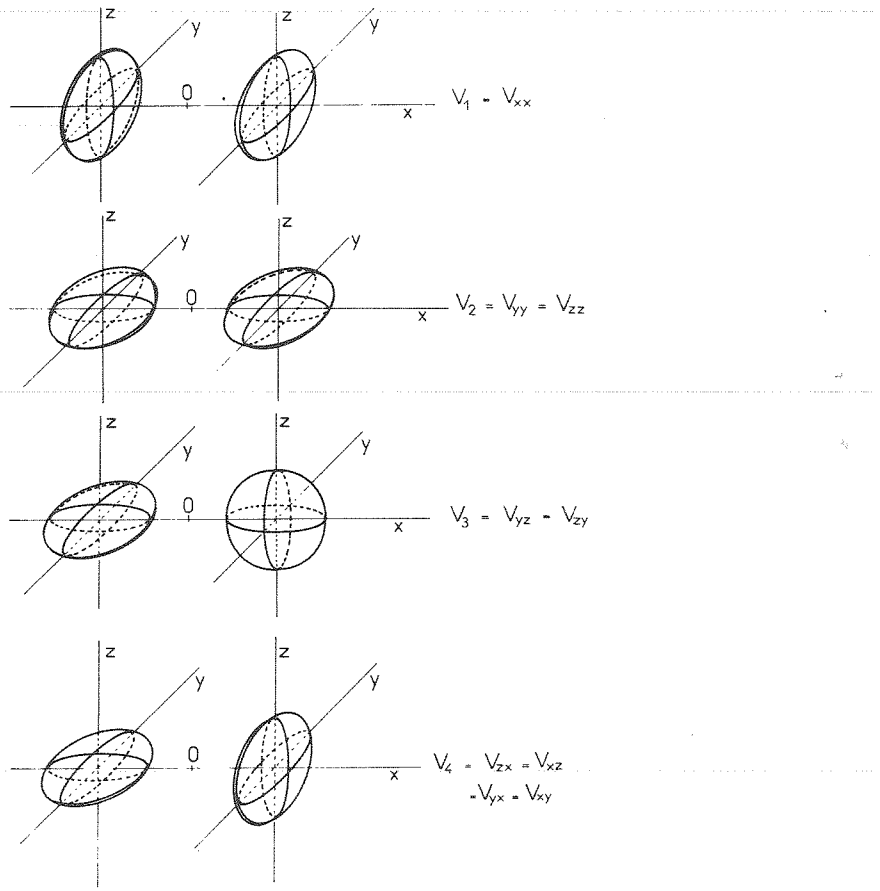

Fig. 1. Diagrams showing the several configurations of the $^{12}C+^{12}C$ system considered in this paper.

curves correspond therefore to a sudden collision with respect to the single-particle quantum numbers. On the other hand our choice of the HF solution implies the adiabaticity with respect to changes of the spatial structure of the nucleon wave functions. The underlying physical assumption is that it is easier for the wave-functions to adjust their shape during the restricted time of a collision than to change their symmetry properties (i.e. number of nodes).

The collective coordinate relevant for the study of a collision is the distance between the two ions. In this work we have studied the CHF energy of the $^{12}C+^{12}C$ system using a constraint on the total quadrupole moment Q and we have defined the distance R between the ions as

$$R = \left(\frac{Q-2Q_{fx}}{A_f}\right)^{\frac{1}{2}}, \tag{1}$$

where Q_{fx} is the quadrupole moment of a single ^{12}C measured along the x-axis.

When the collision takes place according to diagram 1 of fig. 1, $Q_{fx} = Q_f = -39$ fm^2. When configuration 2 is used $Q_{fx} = -\frac{1}{2}Q_f = 19.5$ fm^2. Here A_f stands for the mass number of a fragment (here $A_f = 12$).

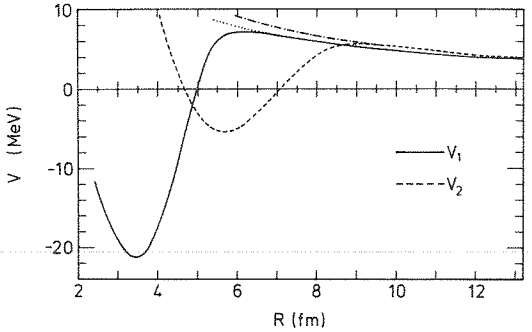

Fig. 2. Constrained HF energy curves. Potentials V_1 and V_2 correspond to the configurations of the $^{12}C+^{12}C$ system shown on the diagrams 1 and 2 of fig. 1. The dotted curve and the dash-dot curve indicate the classical coulomb energies for the configurations 1 and 2 respectively.

In fig. 2 we present our results. The quantities plotted in ordinate are the potentials $V(R)$ defined as the difference between the CHF energy $E(R)$ at a given distance R and the asymptotic value $E(\infty)$. The two potential curves are quite different. For large values of R the difference arises from Coulomb quadrupole-monopole and quadrupole-quadrupole interactions, which differ according to the considered configuration. As expected, Coulomb polarisation effects are small and the HF curves closely reproduce the classical Coulomb values. When R decreases the nuclear interaction sets in first for the triaxial configuration. A minimum of V_2 is reached at $R = 6$ fm, then nuclear repulsion takes place and the system approaches a particle-hole excited configuration of ^{24}Mg. The existence of this minimum at $R = 6$ fm is in keeping with the results of the analysis of ref. [24]). When the two ^{12}C nuclei face each other the top of the barrier occurs at a smaller distance ($R_1 = 6.0$ fm instead of $R_2 = 9.2$ fm) and a higher energy ($V_1 = 7.2$ MeV instead of $V_2 = 5.6$ fm). inside the barrier the potential deepens until a slightly excited ($E_{ex} < 2$ MeV) configuration of ^{24}Mg is reached †.

We shall not try to compare our results with the presently available phenomenological and theoretical potentials. Indeed, we think that such a comparison would not be meaningful since these potentials are used in formalisms quite different from ours ††.

† The HF lowest solution for ^{24}Mg is triaxial. It is not reached, either in V_1 nor V_2, because it corresponds to a different set of quantum numbers.

†† A HF potential for the axial configuration is also calculated in ref. [25]). However a detailed comparison with our results is made difficult by the fact that the authors only give a Saxon-Woods fit to the outer tail of the self-consistent potential.

3. A model for the $^{12}C+^{12}C$ collision

The potential curves obtained above correspond to very specific geometries of the collision. We expect deformed objects like the ^{12}C nuclei to rotate and generate a rotational band. Hence the physical quantity of interest is the interaction energy between two ions with definite angular momentum. In this section we show how it is possible to extract such quantities out of the CHF curves. As a first step we generate in a simple way the wave functions of the 0^+ and 2^+ states of ^{12}C and indicate the relationship of our approximation with the Peierls-Yoccoz method. Second we derive from the CHF curves the potentials between two ions with definite angular momentum in a frame where the line joining the two fragments is at rest, i.e, in what is usually called the rotating frame. At this point we discuss the Born-Oppenheimer approximation. Finally we write the equations in a c.m. frame with fixed axes.

3.1. ROTATION OF A FRAGMENT

In this subsection we consider one ^{12}C nucleus. Let $|x\rangle$, $|y\rangle$ and $|z\rangle$ denote the HF ground states with a symmetry axis pointing in the x, y and z direction. Since, as we shall see later, these three states are orthogonal, we can construct the following three orthogonal vectors,

$$\begin{aligned} |0 \quad 0\rangle &= \sqrt{\tfrac{1}{3}}(|x\rangle+|y\rangle+|z\rangle), \\ |2 \quad 0\rangle &= \sqrt{\tfrac{1}{6}}(2|x\rangle-|y\rangle-|z\rangle), \\ |2\pm 2\rangle &= \sqrt{\tfrac{1}{2}}(|y\rangle-|z\rangle). \end{aligned} \tag{2}$$

The vectors defined in formula (2) should be understood as approximations of the states of good angular momentum obtained according to the Peierls-Yoccoz prescription [26]. Indeed these projected states with angular momentum j and projection m read

$$|jm\rangle = \int \mathrm{d}\Omega D^{j*}_{m0}(\Omega)|\Omega\rangle, \tag{3}$$

where $|\Omega\rangle$ indicates the HF state with its axis pointing in the direction Ω and $D^j_{mm'}(\Omega)$ the usual rotation matrix. The replacement of the integral (3) by a six-point formula [27] with the points $(\theta, \phi) = (0, \phi), (\pi, \phi), (\frac{1}{2}\pi, 0), (\frac{1}{2}\pi, \frac{1}{2}\pi), (\frac{1}{2}\pi, \pi), (\frac{1}{2}\pi, \frac{3}{2}\pi)$ leads to formula (2) for the 0^+ and 2^+ states. In the case of a ^{12}C nucleus, eq. (2) is a rather good approximation. Indeed the overlap $\langle\Omega|\Omega'\rangle$ is a slowly varying function of the angle Θ between the directions Ω and Ω'. For a ^{12}C Slater determinant built with deformed oscillator wave functions one finds

$$\begin{aligned} \langle\Omega|\Omega'\rangle &= \left(\frac{4q}{(1+q)^2-(1-q)^2\cos^2\Theta}\right)^6\left(\frac{4q\cos\Theta}{(1+q)^2-(1-q)^2\cos^2\Theta}\right)^4 \\ &\sim \cos^4\Theta, \end{aligned} \tag{4}$$

where q is the ratio $\omega_\perp/\omega_{||}$ between the oscillator frequency in the plane perpendicular to the ^{12}C symmetry axis ($\omega_\perp$) and the frequency along this axis ($\omega_{||}$). As a consequence of the slow variation of the overlap function, it is not necessary to include in the integral (3) all the directions $|\Omega\rangle$ since most of them would bring in redundant information †. For a heavier system the overlap function decreases much faster and the approximation (2) becomes worse. We should also mention that, with this six-point method, we can describe only two states of a rotational band and cannot distinguish between the states $j = 2$, $m = 2$ and $j = 2$, $m = -2$. From now on we shall assign the state $|00\rangle$ to the ground state of ^{12}C and the states $|20\rangle$ and $|2\pm2\rangle$ to the 2^+ excited state with energy $\Delta E = 4.439$ MeV.

As in other works [17]) we consider the ^{12}C nucleus as a rigid rotor. This approximation is supported by ref. [28]), which evaluates the quantum of quadrupole vibration as large as 7 MeV. In addition the present work does not exclude the polarisation of the intrinsic state of the fragments during the collision, an effect which is actually contained in the curves V_1 and V_2. We only assume that this does not perturb the rotational properties of the fragments.

3.2. BASIS FOR THE TWO-ION SYSTEM; HAMILTONIAN OF INTERACTION

As a basis for the total system, we take the tensor product of the basis of each ^{12}C nucleus. We can label it $\{|x_1x_2\rangle, |x_1y_2\rangle \ldots \ldots |z_1z_2\rangle\}$ or $\{|j_1m_1j_2m_2\rangle\}$. Each HF configuration like $|x_1y_2\rangle$ can be followed continuously for any value of R, and, with the help of the tensor square of the unitary matrix (2), we define the associated states $\{|j_1m_1j_2m_2\rangle\}$. In principle, the second labelling is only meaningful for large distances when the two ions are clearly separated, and have good individual angular momenta. Since we are mainly interested in calculating cross sections, it is sufficient to have a basis whose vectors have a physical meaning asymptotically. However, as will become clear from our definition of the hamiltonian, we will assume that the vectors $|j_1m_1j_2m_2\rangle$ describe, for any distance, states such that both ^{12}C nuclei have a good angular momentum.

Let us now construct the Hamiltonian of interaction H_I, namely the total Hamiltonian H minus the relative kinetic energy. We write it as:

$$H_I = h_1 + h_2 + v(R), \tag{5}$$

where the h_i's are the internal Hamiltonians of the two ^{12}C and $v(R)$ the potential interaction. To be more precise from now on the adjective "internal" will refer only to the orientation coordinates of the fragments and no longer to other nucleonic degrees of freedom inside each fragment. As said in the preceding subsection, the effects of these degrees of freedom is contained in the self-consistent potentials $v(R)$. In the basis $|j_1m_1j_2m_2\rangle$, h_1 is diagonal with eigenvalue 0 for the states $|00, j_2m_2\rangle$

† In the case of oscillator wave functions 15 points are enough to make the integration (3) exact.

and $\Delta E = 4.43$ MeV for the states $|2m_1 j_2 m_2\rangle$. A similar definition holds, of course, for h_2. As for v, we shall neglect its non-diagonal matrix elements in the basis $\{|x_1 x_2\rangle, \ldots |z_1 z_2\rangle\}$. The physical meaning associated with this appproximation is that the interaction v cannot change the orientation of the fragments [†]. Such a change takes place only indirectly via the internal hamiltonians h_i which mix all orientations (they have non-diagonal terms in the basis $\{|x_1 x_2\rangle, \ldots |z_1 z_2\rangle\}$). On the contrary, v, which is non-diagonal in the basis $\{|j_1 m_1 j_2 m_2\rangle\}$ induces angular momentum transfers. Due to the axial symmetry of the ^{12}C nuclei, $v(R)$ has only four distinct eigenvalues. The corresponding configurations are given in fig. 1. To an axial collision (first diagram) corresponds the potential

$$V_{xx}(R) = \langle xx|v(R)|xx\rangle = V_1(R), \tag{6}$$

and to the triaxial configuration 2 two identical potentials depending on whether the ^{12}C axes point in the y- or z-direction,

$$V_{yy}(R) = V_{zz}(R) = V_2(R). \tag{7}$$

We have not calculated the potentials V_3 and V_4 (see fig. 1) which imply the breaking of the $x = 0$ plane symmetry. In the numerical calculations and some discussions we shall replace them by the following approximations

$$V_3 \approx V_2, \qquad V_4 \approx \tfrac{1}{2}(V_1 + V_2). \tag{8}$$

For reasons of geometry these approximations appear reasonable. One can also check that they are exact for the first two leading terms of the Coulomb interaction (monopole-monopole, monopole-quadrupole).

We are now able to write the Hamiltonian H_I in the $\{|j_1 m_1 j_2 m_2\rangle\}$ basis but we will first make a study of its symmetries.

3.3. THE SYMMETRIES OF H_I

We shall make use of the analogy of our model with those commonly used in molecular physics [30]). In the rotating frame[††] we distinguish four types of symmetries:

(i) H_I is invariant with respect to any rotation around the line joining the two c.m.s. (the invariant line). The quantum number associated with this symmetry is the projection $\Lambda = m_1 + m_2$ of the total *internal* angular momentum on the invariant line.

(ii) A reflexion through any plane containing the invariant line leaves H_I unchanged. However in our case this symmetry does not induce any simplifications of H_I in addition to those introduced by (i).

[†] This is in good agreement with the results of semiclassical calculations of heavy-ion collisions [29]).

[††] As usual this frame is chosen so that the c.m. of the two ^{12}C always lie on its Ox axis. The potentials V_i have been defined in this frame.

TABLE 1

Matrix elements of the interaction Hamiltonian H_1 on the symmetric and antisymmetric basis $|(j_1m_1)(j_2m_2)c\rangle$ (c = a or s)

	$\|(00)(00)s\rangle$	$\|(00)(20)s\rangle$	$\|(20)(20)s\rangle$	$\|(22)(2-2)s\rangle$	$\|(00)(20)s\rangle$
$\|(00)(00)s\rangle$	$\frac{1}{9}(V_1+2V_2+2V_3+4V_4)$	$\frac{2}{9}(V_1-V_2-V_3+V_4)$	$\frac{1}{9}(2V_1+V_2+V_2-4V_4)$	$\frac{1}{3}(V_2-V_3)$	0
$\|(00)(20)s\rangle$	$\frac{2}{9}(V_1-V_2-V_3+V_4)$	$\frac{1}{9}(4V_1+2V_2+2V_3+V_4)+\Delta E$	$\frac{1}{9}(4V_1-V_2-V_3-2V_4)$	$\frac{1}{3}(V_3-V_2)$	0
$\|(20)(20)s\rangle$	$\frac{1}{9}(2V_1+V_2+V_3-4V_4)$	$\frac{1}{9}(4V_1-V_2-V_3-2V_4)$	$\frac{1}{18}(8V_1+V_2+V_3+8V_4)+2\Delta E$	$\frac{1}{6}(V_2-V_3)$	0
$\|(22)(2-2)s\rangle$	$\frac{1}{3}(V_2-V_3)$	$\frac{1}{3}(V_3-V_2)$	$\frac{1}{6}(V_2-V_3)$	$\frac{1}{2}(V_2+V_3)+2\Delta E$	0
$\|(00)(20)a\rangle$	0	0	0	0	$V_4+\Delta E$

	$\|(00)(22)s\rangle$	$\|(20)(22)s\rangle$	$\|(00)(22)a\rangle$	$\|(20)(22)a\rangle$
$\|(00)(22)s\rangle$	$\frac{1}{3}(2V_2+V_4)+\Delta E$	$\frac{1}{3}\sqrt{2}(V_4-V_2)$	0	0
$\|(00)(22)s\rangle$	$\frac{1}{3}\sqrt{2}(V_4-V_2)$	$\frac{1}{3}(2V_4+V_2)+2\Delta E$	0	0
$\|(00)(22)a\rangle$	0	0	$\frac{1}{3}(2V_3+V_4)+\Delta E$	$\frac{1}{3}\sqrt{2}(V_4-V_3)$
$\|(20)(22)a\rangle$	0	0	$\frac{1}{3}\sqrt{2}(V_4-V_3)$	$\frac{1}{3}(2V_4+V_3)+2\Delta E$

(iii) The Hamiltonian H_I is invariant under an inversion through the c.m. of the total system.

(iv) H_I is left unchanged by the interchange of the coordinates of two ^{12}C nuclei.

Since the last two invariances are preserved when the relative kinetic energy is added to H_I they will induce a symmetry classification of the total wave function that we shall describe later. To make their influence on the structure of H_I visible, we shall introduce the symmetrized basis $\{|(j_1m_1)(j_2m_2)\mathrm{s}\rangle;\ |(j_1m_1)(j_2m_2)\mathrm{a}\rangle\}$ defined as

$$|(j_1,m_1)(j_2,m_2)^{\mathrm{s}}_{\mathrm{a}}\rangle = \frac{1}{\sqrt{2(1+\delta_{j_1j_2}\delta_{m_1m_2})}}(|(j_1,m_1)(j_2,m_2)\rangle \pm |(j_2,m_2)(j_1,m_1)\rangle). \quad (9)$$

In table 1, we give the expression for H_I on the symmetrized basis in terms of the four potentials V_i and the excitation energy ΔE. Table 2 shows how H_I simplifies when the approximation (8) is introduced. Due to our restricted basis we know the Hamiltonian H_I in the subspace $\Lambda = 0,\ \pm 2,\ \pm 4$ only. To pursue our analysis it is easier to introduce states of the $^{12}C+{}^{12}C$ system with definite total internal angular momentum I namely the basis $\{|(j_1j_2)I\Lambda\mathrm{s}\rangle;|(j_1j_2)I\Lambda\mathrm{a}\rangle\}$ with

$$|(j_1j_2)I\Lambda\mathrm{s}\rangle = \sum_{m_1m_2}(j_1m_1j_2m_2|I\Lambda)|(j_1,m_1)|(j_2,m_2)\mathrm{s}\rangle. \quad (10)$$

A similar definition holds for the antisymmetric states. However the sums performed in eq. (10) run over all values of m_1 and include states of ^{12}C like $|j=2,\ m=1\rangle$ which are not in our basis (2). To estimate the missing matrix elements of H_I we make use of geometric considerations: the state $|21\rangle$ of ^{12}C corresponds to an angular momentum pointing 45° aside the invariant line while $|20\rangle$ is essentially aligned with, and $|2\pm2\rangle$ perpendicular to, this line. Hence we shall replace any diagonal matrix element involving $|21\rangle$ like $\langle(21)(2-1)\mathrm{s}|H_I|(21)(2-1)\mathrm{s}\rangle$ by the average between $\langle(20)(20)|H_I|(20)(20)\rangle$ and $\langle(22)(2-2)\mathrm{s}|H_I|(22)(2-2)\mathrm{s}\rangle$ and neglect any off-diagonal term involving states like $|(21)(2-1)\mathrm{s}\rangle$. This prescription is exact for the h_1+h_2 part of H_I and is reasonable for v which is predominantly sensitive to the relative orientation of the fragments.

In table 3 we give its expression in the $\Lambda \geqq 0$ subspaces ($\Lambda < 0$ matrices are identical) of the basis $\{|(j_1j_2)I\Lambda\mathrm{s}\rangle\}$. We do not consider here the antisymmetric subspace $\{|(j_1j_2)I\Lambda\mathrm{a}\rangle\}$ which is not useful for the study of a $^{12}C+{}^{12}C$ collision because the symmetry of the initial state of the collision is not broken by the Hamiltonian.

Several remarks can be made about the structure of H_I. First we note that I is not a good quantum number so that H_I induces rotational excitations of the ^{12}C nuclei. Second all the coupling terms are proportional to the difference $V_1 - V_2$. This was expected since the possibility of a change of the angular momentum arises only from the difference between V_1 and V_2 and disappears when the potentials

TABLE 2

Same as table 1 with approximation (8) taken into account

	$\|(00)(00)s\rangle$	$\|(00)(20)s\rangle$	$\|(20)(22)s\rangle$	$\|(22)(2-2)s\rangle$	$\|(00)(20)a\rangle$
$\|(00)(00)s\rangle$	$\frac{1}{3}(V_1+2V_2)$	$\frac{1}{3}(V_1-V_2)$	0	0	0
$\|(00)(20)s\rangle$	$\frac{1}{3}(V_1-V_2)$	$\frac{1}{2}(V_1+V_2)+\Delta E$	$\frac{1}{3}(V_1-V_2)$	0	0
$\|(20)(22)s\rangle$	0	$\frac{1}{3}(V_1-V_2)$	$\frac{1}{3}(2V_1+V_2)+2\Delta E$	0	0
$\|(22)(2-2)s\rangle$	0	0	0	$V_2+2\Delta E$	0
$\|(00)(20)a\rangle$	0	0	0	0	$\frac{1}{2}(V_1+V_2)+2\Delta E$

	$\|(00)(22)s\rangle$	$\|(20)(22)s\rangle$	$\|(00)(22)a\rangle$	$\|(20)(22)a\rangle$
$\|(00)(22)s\rangle$	$\frac{1}{6}(V_1+5V_2)+\Delta E$	$\frac{1}{6}\sqrt{2}(V_1-V_2)$	0	0
$\|(20)(22)s\rangle$	$\frac{1}{6}\sqrt{2}(V_1-V_2)$	$\frac{1}{3}(V_1+2V_2)+2\Delta E$	0	0
$\|(00)(22)a\rangle$	0	0	$\frac{1}{6}(V_1+5V_2)+\Delta E$	$\frac{1}{6}\sqrt{2}(V_1-V_2)$
$\|(20)(22)a\rangle$	0	0	$\frac{1}{6}\sqrt{2}(V_1-V_2)$	$\frac{1}{3}(V_1+2V_2)+2\Delta E$

TABLE 3

Matrix elements $H_{\Lambda}^{cc'}$ of the interaction Hamiltonian H_1 on the symmetric basis $|(j_1 j_2) I \Lambda s\rangle$

$\Lambda = 0$	$\|(00)00s\rangle$	$\|(20)20s\rangle$	$\|(22)00s\rangle$	$\|(22)20s\rangle$	$\|(22)40s\rangle$
$\|(00)00s\rangle$	$\frac{1}{3}(V_1+2V_2)$	$\frac{1}{3}(V_1-V_2)$	0	0	0
$\|(20)20s\rangle$	$\frac{1}{3}(V_1-V_2)$	$\frac{1}{2}(V_1+V_2)+\Delta E$	$\frac{1}{3}\sqrt{\frac{1}{5}}(V_1-V_2)$	$-\frac{1}{3}\sqrt{\frac{7}{7}}(V_1-V_2)$	$\sqrt{\frac{2}{35}}(V_1-V_2)$
$\|(22)00s\rangle$	0	$\frac{1}{3}\sqrt{\frac{1}{5}}(V_1-V_2)$	$\frac{1}{15}(4V_1+11V_2)+2\Delta E$	$-\sqrt{\frac{2}{35}}(V_1-V_2)$	$\frac{2}{3}\sqrt{\frac{2}{175}}(V_1-V_2)$
$\|(22)20s\rangle$	0	$-\frac{1}{3}\sqrt{\frac{7}{7}}(V_1-V_2)$	$-\sqrt{\frac{2}{35}}(V_1-V_2)$	$\frac{1}{21}(5V_1+16V_2)+2\Delta E$	$-\frac{8}{3}\sqrt{\frac{1}{245}}(V_1-V_2)$
$\|(22)40s\rangle$	0	$\sqrt{\frac{2}{35}}(V_1-V_2)$	$\frac{2}{3}\sqrt{\frac{2}{175}}(V_1-V_2)$	$-\frac{8}{3}\sqrt{\frac{1}{245}}(V_1-V_2)$	$\frac{1}{105}(52V_1+53V_2)+2\Delta E$

$\Lambda = 1$	$\|(02)21s\rangle$	$\|(22)21s\rangle$	$\|(22)41s\rangle$
$\|(0221s\rangle$	$\frac{1}{3}(V_1+2V_2)+\Delta E$	0	0
$\|(22)21s\rangle$	0	$\frac{1}{14}(3V_1+11V_2)+2\Delta E$	$-\frac{1}{21}\sqrt{6}(V_1-V_2)$
$\|(22)41s\rangle$	0	$-\frac{1}{21}\sqrt{6}(V_1-V_2)$	$\frac{1}{42}(19V_1+23V_2)+2\Delta E$

$\Lambda = 2$	$\|(02)22s\rangle$	$\|(22)(22s\rangle$	$\|(22)42s\rangle$
$\|(02)22s\rangle$	$\frac{1}{6}(V_1+5V_2)+\Delta E$	$\frac{2}{3}\sqrt{\frac{1}{14}}(V_1-V_2)$	$\sqrt{\frac{1}{42}}(V_1-V_2)$
$\|(22)22s\rangle$	$\frac{2}{3}\sqrt{\frac{1}{14}}(V_1-V_2)$	$\frac{1}{3}(V_1+2V_2)+2\Delta E$	0
$\|(22)42s\rangle$	$\sqrt{\frac{1}{42}}(V_1-V_2)$	0	$\frac{1}{3}(V_1+2V_2)+2\Delta E$

$\Lambda = 3$	$\|(22)43s\rangle$
$\|(22)43s\rangle$	$\frac{1}{6}(V_1+5V_2)+2\Delta E$

$\Lambda = 4$	$\|(22)44s\rangle$
$\|(22)44s\rangle$	$V_2+2\Delta E$

become identical. On the other hand, one notes that there is no direct coupling of the elastic channel to the double inelastic channel. This is a consequence of the approximation (8) which does not hold when the four potentials V_i are used.

3.4. EQUATIONS OF MOTION IN THE ROTATING FRAME; BORN-OPPENHEIMER POTENTIALS

The full Hamiltonian of the system reads:

$$H = -\frac{\hbar^2}{2\mu}\Delta + H_1. \tag{11}$$

In formula (11), the first term is the relative kinetic energy and μ is the reduced mass. In order to derive the dynamical equations we proceed as usual. We study the action of the Hamiltonian H on the most general collision wave function written in the rotating frame and deduce a set of coupled equations for the several radial amplitudes. Hereafter we shall use the shorthand notation c to label the quantum numbers (j_1, j_2, I) of the internal states of the $^{12}C+^{12}C$ system and denote $H^{cc'}_{\Lambda}$ the matrix element

$$H^{cc'}_{\Lambda} = \langle (j_1 j_2) I \Lambda s | H_1 | (j'_1 j'_2) I' \Lambda s \rangle. \tag{12}$$

The most general expression of a scattering wave function in the rotating frame can be written as

$$\psi = \sum_J (2J+1) \sum_{\Lambda c} \frac{1}{R} \eta^{JM}_{c\Lambda}(k_c R) D^{J*}_{M\Lambda}(\phi, \theta, 0) | c\Lambda \rangle. \tag{13}$$

In formula (13) $\eta^{JM}_{c\Lambda}(k_c R)$ is the radial relative wave function, $D^J_{M\Lambda}$ is the rotation matrix, θ and ϕ are the two Euler angles which bring the fixed OX axis onto the invariant line Ox and Λ labels, as above, the projection of the internal angular momentum on the invariant line.

We are now in position to study the action of H on ψ. The Hamiltonian can be split in three terms:

$$H = H_1 - \frac{\hbar^2}{2\mu} \frac{1}{R} \frac{\partial^2}{\partial R^2} R + \frac{\hat{L}^2 \hbar^2}{2\mu R^2}. \tag{14}$$

In the evaluation of $H\psi$ only the third term of H gives rise to some difficulties.

To study the action of the orbital angular momentum $\hat{L}^2$ we shall write it as

$$\hat{L}^2 = \hat{J}^2 + \hat{I}^2 - 2\hat{J} \cdot \hat{I}, \tag{15}$$

where we have introduced the total angular momentum operator $\hat{J}$ and the internal angular momentum operator $\hat{I}$. The problem is now identical to that encountered in the rotational model from which we can extract the solution [31]). After having collected the three contributions to $H\psi$ and projected onto $D^J_{M\Lambda}|c\Lambda\rangle$ we find the

coupled radial equations

$$\left(\frac{d^2}{dR^2} - \frac{J(J+1)+I(I+1)-2\Lambda^2}{R^2} + k^2\right)\eta_{c\Lambda}^{JM} - \frac{2\mu}{\hbar^2}\sum_{c'} H_{\Lambda}^{cc'}(R)\eta_{c'\Lambda}^{JM}$$
$$-\left[(J(J+1)-(\Lambda+1)\Lambda)(I(I+1)-(\Lambda+1)\Lambda)\right]^{\frac{1}{2}}\eta_{c\Lambda+1}^{JM}$$
$$-\left[(J(J+1)-(\Lambda-1)\Lambda)(I(I+1)-(\Lambda-1)\Lambda)\right]^{\frac{1}{2}}\eta_{c\Lambda-1}^{JM} = 0. \tag{16}$$

In eq. (16), the last two terms are due to the Coriolis coupling. They are responsible for the breaking of the Λ-symmetry. In molecular physics a well-known approximation to this set of equations is the so-called Born-Oppenheimer method [30]), which neglects the Coriolis coupling and introduces a R-dependent basis diagonalizing the interaction matrix $H_{\Lambda}^{cc'}(R)$ for every value of the separation distance R. If we consider the block $\Lambda = 0$, this diagonalization can be done analytically. The lowest Born-Oppenheimer potential (elastic channel) is

$$\varepsilon_1(R) = \tfrac{1}{2}(V_1+V_2)+\Delta E-\left[\tfrac{1}{4}(V_1-V_2)^2+\tfrac{1}{3}\Delta E(V_1-V_2)+(\Delta E)^2\right]^{\frac{1}{2}}. \tag{17}$$

When $\Delta E \to 0$ $\varepsilon_1(R)$ reduces to $\mathrm{Inf}(V_1, V_2)$. One may note that $\mathrm{Inf}(V_1, V_2)$ has already been used in ref. [32]) although the connection with the Born-Oppenheimer method had not been emphasized. When $\Delta E \to \infty$, $\varepsilon_1(R) \to \frac{1}{3}(V_1+2V_2)$ which, as we shall see in subsect. 3.5, is the elastic potential of the system of coupled equations in the fixed frame. This is not surprising since the problem reduces to a description of simple elastic scattering when the internal excitation energy goes to infinity. The combination V_1+2V_2 is such that the monopole-quadrupole terms ($\sim R^{-3}$) of the Coulomb potential disappear so that the potential for large R-values is a pure point Coulomb potential as should be expected for the interaction of 0^+ states.

In fig. 3 we compare the potentials V_1, V_2 and the Born-Oppenheimer potentials $\varepsilon_{1,2}$ which asymptotically correspond to the elastic and simple inelastic channels. We have subtracted the point Coulomb interaction from all the potentials. From this figure, one can check that the Born-Oppenheimer approximation fails in molecular nuclear physics. Indeed a simple estimate shows that the energy difference between the vibrational states in the potential wells $\varepsilon_i(R)$ has the same order of magnitude as the separation between these wells. Hence a discussion in terms of one Born-Oppenheimer potential is not possible and a solution of the full coupled system (16) becomes necessary.

3.5. EQUATIONS OF MOTION IN A FIXED FRAME

To write the equation in a fixed frame, we start from the general expression of a scattering wave ψ with total angular momentum J and projection M on the beam axis,

$$\psi_{JM} = \sum_{lc}\frac{1}{R}\chi_{cl}^{J}(R)\left[Y_l^{M_l}\otimes|cM_1\rangle\right]_M^J. \tag{18}$$

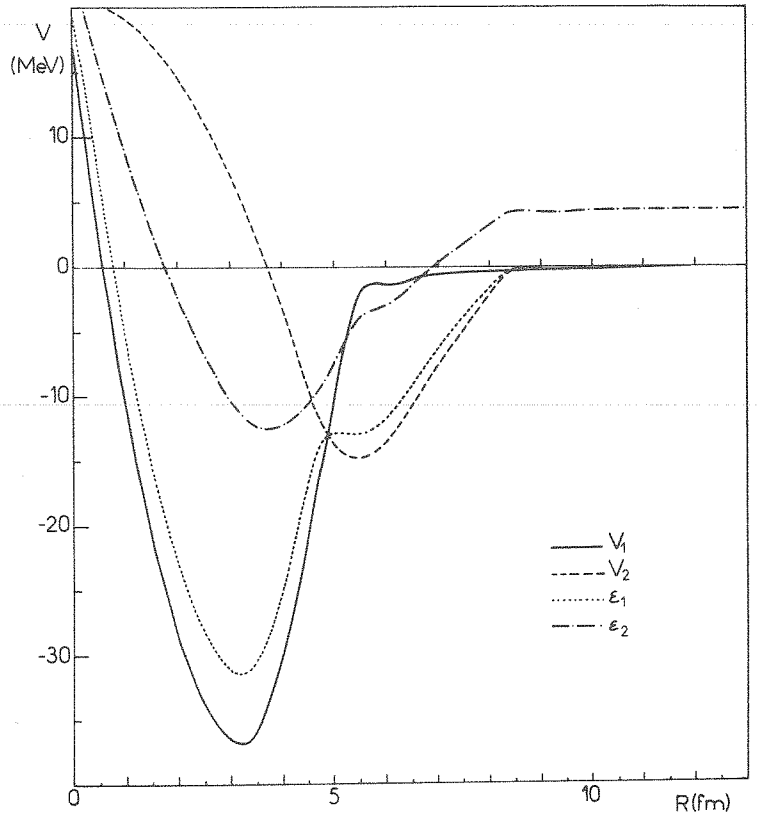

Fig. 3. Born-Oppenheimer potentials ε_1 and ε_2 associated respectively with the elastic and single inelastic channels.

It will now be convenient to introduce the notation $\bar{c}$ for the set of quantum numbers $\{cl\}$. The coupled set of equations for the radial wave functions $\chi^J_{\bar{c}}(R)$ is

$$\left(\frac{\mathrm{d}^2}{\mathrm{d}R^2} - \frac{l(l+1)}{R^2} + k^2\right)\chi^J_{\bar{c}}(R) - \frac{2\mu}{\hbar^2}\sum_{\bar{c}'} V^{\bar{c}\bar{c}'}(R)\chi^J_{\bar{c}'}(R) = 0, \tag{19}$$

where we have introduced the notation

$$V^{\bar{c}\bar{c}'}(R) = \langle [Y_l^{M_l} \otimes |cM_I\rangle]^J_M | H_I | [Y_{l'}^{M_{l'}} \otimes |c'M_I\rangle]^J_M \rangle. \tag{20}$$

In order to evaluate the matrix element $V^{\bar{c}\bar{c}'}$ we need the expression of the state $[Y_l^{M_l} \otimes |cM_I\rangle]^J_M$ in the rotating frame:

$$[Y_l^{M_l} \otimes |cM_I\rangle]^J_M = \sum_\Lambda (-1)^{l-I+M}\sqrt{(2J+1)(2l+1)/4\pi} \times \begin{pmatrix} l & I & J \\ 0 & \Lambda & -\Lambda \end{pmatrix} D^J_{-M-\Lambda}(\phi, \theta, 0)|c\Lambda\rangle. \tag{21}$$

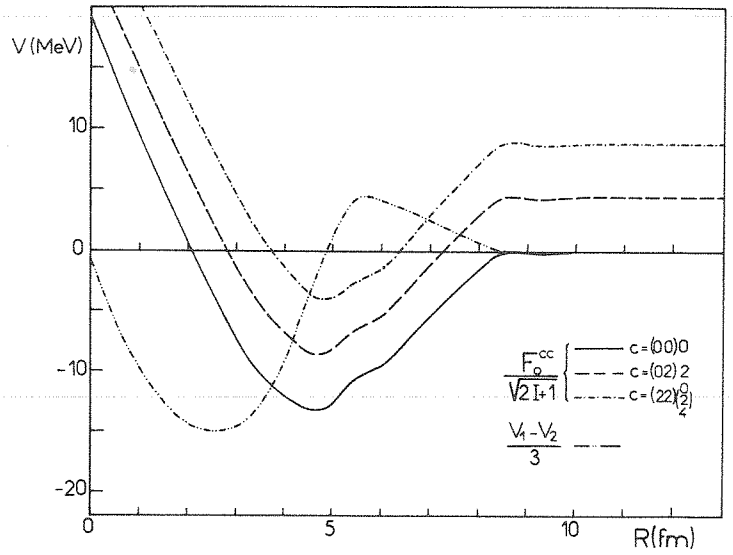

Fig. 4. Potentials and coupling factor (eq. (24)) for the $^{12}C+^{12}C$ system.

After some straightforward angular coupling algebra, one finds the expressions of $V^{\overline{cc'}}$ in terms of the $H_\Lambda^{cc'}$s †:

$$V^{\overline{cc'}}(R) = ((2l+1)(2l'+1))^{\frac{1}{2}}(-1)^J \sum_\lambda (-1)^\lambda (2\lambda+1)$$

$$\times \begin{pmatrix} l & l' & \lambda \\ 0 & 0 & 0 \end{pmatrix} \begin{Bmatrix} l & I & J \\ I' & l' & \lambda \end{Bmatrix} F_\lambda^{cc'}(R),$$

$$F_\lambda^{cc'}(R) = \sum_\Lambda (-1)^\Lambda \begin{pmatrix} I & I' & \lambda \\ \Lambda & -\Lambda & 0 \end{pmatrix} H_\Lambda^{cc'}(R). \tag{22}$$

In the above formula the $F_\lambda^{cc'}$s are the reduced matrix elements leading to a transfer of angular momentum λ between the internal states c and c' ††. We list them in table 4. All the off-diagonal elements as well as the diagonal elements F_λ^{cc} with $\lambda \neq 0$ are proportional to $V_1 - V_2$. In fig. 4 we display the three distinct diagonal elements $F_0^{cc}/\sqrt{2I+1}$ (the so-called channel potentials) and the coupling factor $\frac{1}{3}(V_1 - V_2)$. Except for an energy shift the three potentials are very similar. Interesting to note is the strength and the R-dependence of the coupling factor $(V_1 - V_2)$ which as we shall see induce large inelastic and double inelastic cross sections.

† The geometrical factors in front of eq. (22) differ from some of those available in the literature by a factor $i^{\lambda+l+l'}$ because we used throughout this paper the phase convention of Brink and Satchler [33]) instead of that of Rose [34]).

†† For the numerical applications the Coulomb potential has been included in the coefficients $F_\lambda^{cc'}(R)$ and $V^{cc'}(R)$, eqs. (19) and (22).

The coupled systems (19) and (16) are equivalent. If one neglects Coriolis coupling eqs. (16) become much easier to solve. However the handling of the asymptotic conditions in the rotating frame requires some care. For this reason and because a standard coupled channel code was at our disposal we have rather solved eq. (19). Because of the symmetry under the interchange of the coordinate of the two fragments only even partial waves l and l' occur. In addition the scattering amplitude must be symmetrized.

4. Results

Up to now the matrix elements $V^{\overline{cc}'}$ have been expressed in terms of the microscopically calculated quantities V_1 and V_2. However our model includes only three of the possible channels. In order to reproduce the reaction cross section we need some absorption; in other word an imaginary potential. We first discuss how this potential was chosen, then present our results.

4.1. ABSORPTION POTENTIAL

With the possible exception of the α-particle channels [35]), it is generally believed that most of the inelastic channels not included here are fed by compound nuclear process. This means generally a fusion of the two partners or at least a large overlap.

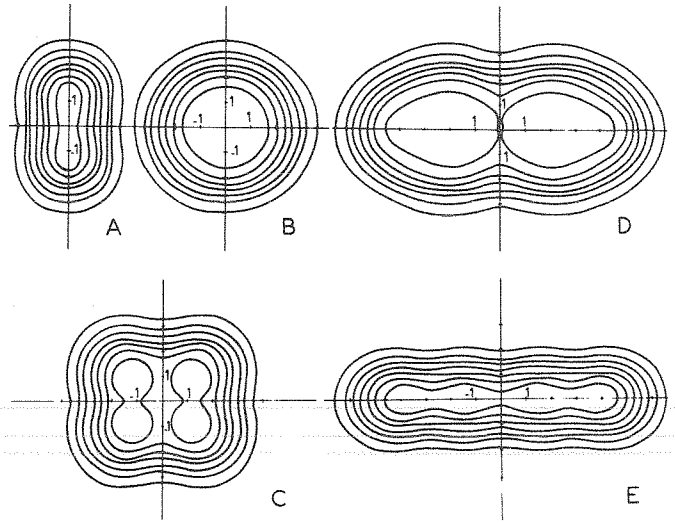

Fig. 5. Contour lines of the total density. (A) ^{12}C ground state density in plane passing through the symmetry axis, (B) the plane of the figure is perpendicular to the symmetry axis, (C) density of the axial configuration of the $^{12}C+^{12}C$ system in the plane $z = 0$ (see diagram 1, fig. 1) for the value of R corresponding to the minimum of V_1, (D) density of the triaxial configuration of the $^{12}C+^{12}C$ system in the plane $z = 0$ (see diagram 2, fig. 1) for the value of R corresponding to the minimum fo V_2, (E) same as D for the plane $y = 0$. Each contour line indicates a 0.02 fm^{-3} increase of the density.

TABLE 4

Reduced matrix elements $F_\lambda^{cc'}$ of the interaction Hamiltonian (see text)

$c = (00)0$		$c = (02)2$		$c = (22)0$		$c = (22)2$		$c = (22)4$		
0	$\frac{1}{3}(V_1+2V_2)$	*2*	$\frac{1}{3}\bar{V}$	*0*	0	*2*	0	*4*	0	$c = (00)0$
		0	$\sqrt{5}\frac{1}{10}(3V_1+7V_2)+\Delta E$	*2*	$\frac{1}{3}\sqrt{\frac{1}{5}}\bar{V}$	*0*	$\frac{2}{3}\sqrt{\frac{1}{70}}\bar{V}$	*2*	$\frac{11}{105}\sqrt{5}\bar{V}$	
		2	$-\sqrt{\frac{1}{14}}\bar{V}$			*2*	$\frac{2}{7}V$	*4*	$\frac{1}{7}\sqrt{\frac{2}{11}}\bar{V}$	$c = (02)2$
		4	$\frac{2}{3}\sqrt{\frac{1}{70}}\bar{V}$			*4*	$-\frac{4}{21}\sqrt{\frac{1}{5}}\bar{V}$	*6*	$\frac{4}{3}\sqrt{\frac{2}{77}}\bar{V}$	
				0	$\frac{1}{15}(4V_1+11V_2)+2\Delta E$	*2*	$-\sqrt{\frac{2}{35}}\bar{V}$	*4*	$\frac{2}{15}\sqrt{\frac{2}{7}}\bar{V}$	$c = (22)0$
						0	$\sqrt{5}\frac{1}{15}(4V_1+11V_2)+2\Delta E$	*2*	$-\frac{6}{7}\sqrt{\frac{2}{35}}\bar{V}$	
						2	$\frac{3}{7}\sqrt{\frac{1}{14}}\bar{V}$	*4*	$\frac{22}{21}\sqrt{\frac{1}{77}}\bar{V}$	$c = (22)2$
						4	$\frac{8}{21}\sqrt{\frac{1}{70}}\bar{V}$	*6*	0	
								0	$3\ \frac{1}{15}(4V_1+11V_2)+2\Delta E$	
								2	$-\frac{3}{7}\sqrt{\frac{11}{7}}\bar{V}$	
								4	$\frac{1}{105}\sqrt{\frac{286}{7}}\bar{V}$	$c = 22(4)$
								6	0	
								8	0	

We give first λ (in italics), then $F_\lambda^{cc'}$. $\bar{V} = V_1 - V_2$.

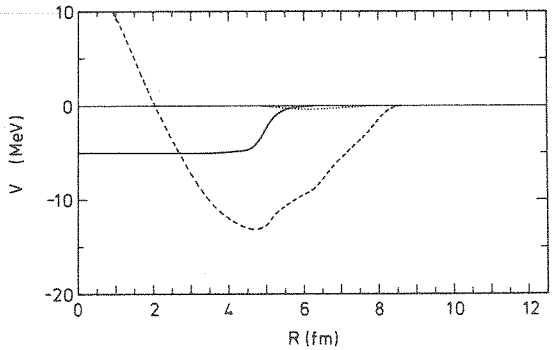

Fig. 6. The full line curve is the imaginary part added to the elastic potential (dashed curve). The imaginary potential has a range smaller than that of potential V_1 (fig. 2). The dotted curve shows for comparison the imaginary potential used in ref. [16]).

According to fig. 2 it is natural to associate the compound nuclear formation to a collision in the axial configuration (potential V_1). Indeed the minimum of V_1 corresponds to a fused system close to the ground state of ^{24}Mg †. On the contrary in the triaxial mode the nuclear saturation creates a repulsion for distances smaller than 6 fm before any strong mixing of the two ions can take place. This can be seen in fig. 5 where the nuclear density in the equatorial plane of the two ^{12}C is shown for a distance of the two ^{12}C corresponding to the minima of V_1 and V_2. We shall therefore introduce an imaginary part with range slightly smaller than that of V_1 and add it to V_1 everywhere this potential appears in the reduced matrix elements and potentials of the coupled equations (table 4). This procedure leads to complex coupling terms. It is sometimes argued on the basis of statistical assumptions that the coupling terms should be real. However the validity of these assumptions is questionable for strongly correlated channels (i.e., channels with very similar intrinsic wave functions), as the ones built on the rotational states described here [36]). We would like also to mention that complex coupling is often used in phenomenological analysis [37]), at least for nucleon channels. In any case, the complex coupling terms in our model arise naturally from the geometrical relationship (see eqs. (2) and (3)) between the different channels.

All the results presented hereafter have been obtained with a Woods-Saxon imaginary potential of radius $R = 5$ fm and surface width $a = 0.2$ fm. The depth of the potential has been roughly adjusted to give good average agreement with the experimental fusion cross sections ††. In fig. 6, we show the imaginary potential (depth of 5 MeV) added to the elastic potential $V^{\bar{0}\bar{0}}(R)$ along with $V^{\bar{0}\bar{0}}(R)$. As a comparison we give on the same figure the imaginary potential used in ref. [16]). The qualitative

† As said in sect. 2 the HF ground state of ^{24}Mg is triaxial, but its energy is less than 2 MeV below that of the minimum of V_1.

†† We define it as the total reaction cross section minus the inelastic channel cross sections.

and quantitative differences are certainly due to our additional requirement of reproducing the fusion data. In fig. 7 we display our results for the fusion cross section. A good agreement is obtained for the highest bombarding energies. At low energy we overestimate the fusion cross section. This indicates that an imaginary potential with depth increasing with energy would be more appropriate in the 5–15 MeV region. However in this paper we shall focus our attention on the qualitative and semi-quantitative implications of our microscopic model and shall not attempt a detailed study of the influence of the phenomenological imaginary potential.

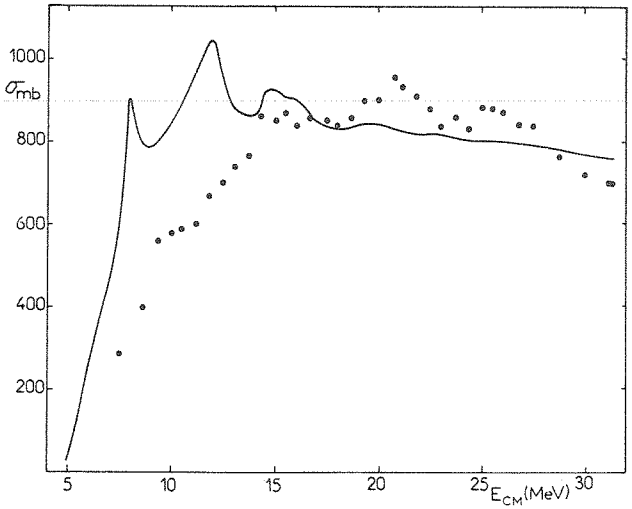

Fig. 7. Experimental (dots) and calculated (full line) total fusion cross section. Data taken from ref. [9]).

Before going into the discussion of the elastic and inelastic cross sections we mention a technical point. The real potentials V_1 and V_2 have been calculated for distances $R > 2.2$ fm and $R > 3.5$ fm respectively. At shorter distances the nuclear saturation of the effective nucleon-nucleon force and the Pauli principle lead to a repulsive core that we did not try to compute in full detail. We have rather extrapolated the curves towards $R = 0$ by means of a parabolic extrapolation. It is our belief that this procedure does not affect sensitively our results. Indeed a precise knowledge of the real potentials at short distances is certainly of small importance in view of the magnitude of the absorptive potential ($V_I \approx 5$ MeV for $R \lesssim 4.7$ fm).

4.2. ELASTIC AND INELASTIC CROSS SECTIONS

Our results for the 90° excitation functions are shown in fig. 8. The general slope of the elastic cross section is correctly reproduced as well as the amplitude of the gross structure oscillations. However the minima of the calculated curve do not always occur at the right energy. We have not studied whether this discrepancy could

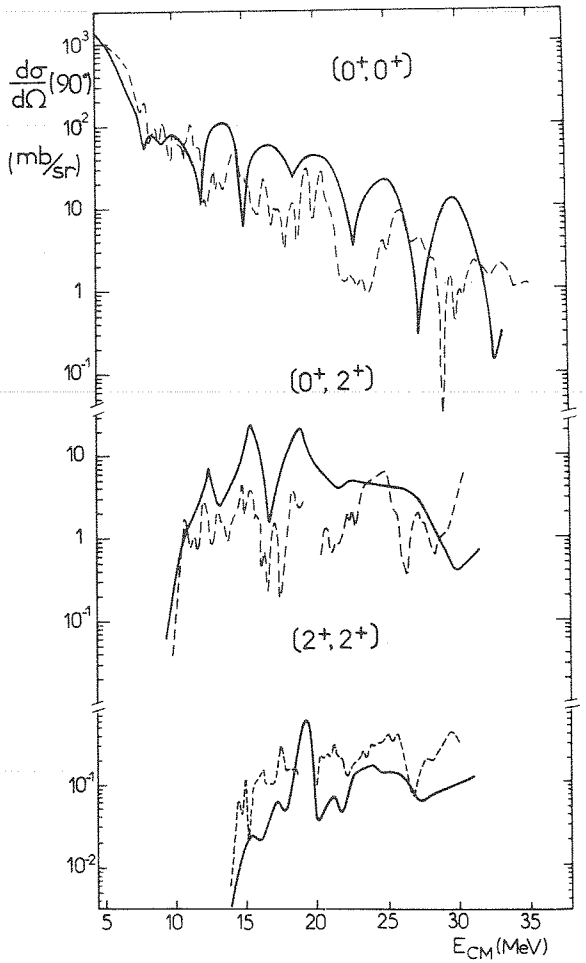

Fig. 8. Experimental (dash) and calculated (full line) excitation functions at 90° for the elastic (0^+0^+) single (0^+2^+) and double inelastic (2^+2^+) channels. Data from refs. [2-6]).

be cured via a better choice of the imaginary potential. The theoretical curve shows no fine structure. In our calculation it is washed out by the strength of the absorption. It is not clear whether the use of a shallower imaginary potential in the 5–15 MeV region as suggested by the comparison with fusion data would reveal any narrow resonances. It therefore seems impossible within our model to explain both the existence of a fine structure in the elastic cross section and the magnitude of the fusion cross section.

The average agreement obtained for the simple and double inelastic yield indicates that the coupling factor ($\sim V_1 - V_2$) predicted by our model has the right order of magnitude. The fact that we slightly underestimate the double inelastic cross section may be due to our use of approximation (8) which restricts the double excita-

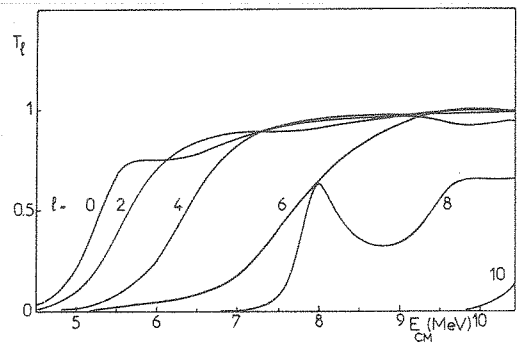

Fig. 9. Transmission factors T_l.

tion to a two-step process (see subsect. 3.3). As was the case for the elastic data, we do not reproduce the experimental fine structure.

To conclude this section we give in fig. 9 the transmission factors for the lowest potential waves in the energy range just above the Coulomb barrier. It can be seen that the first oscillation in the ascending part of the fusion cross section is associated with a resonance in the $l = 8$ partial wave.

5. Conclusion

In this paper we presented a simple model that attempts a microscopic description of the molecular motion for the $^{12}C+^{12}C$ system. Starting from two constrained Hartree-Fock energy curves we were able to explain the magnitude and the main features of the elastic and inelastic cross sections. We could not however explain at the same time the fine structure in these cross sections and the fusion data. It seems to us that most of the available models suffer from the same deficiency and can only explain the first phenomenon by ignoring fusion data. Our discrepancy is certainly an indication that the simple imaginary potential is too crude a model for the description of the absorption even when the (2^+0^+) (2^+2^+) channels are explicitly taken into account.

By an analysis in terms of the Born-Oppenheimer method, we have shown the connection of our model with earlier ones [32]) and discussed the approximations that they contained. Improvements can be achieved in a consistent way along several lines. First, dynamical calculations using the ATDHF method [22]) could tell us how much the collective mass $\mu(R)$ departs from the asymptotic reduced mass value and how the position of potential resonances is affected †. Second, constrained HF calculations with an additional constraint on the total angular momentum ωJ_x ††

† An indication of the magnitude of this effect is given in ref. [38]) where the collective mass is calculated according to the Inglis cranking formula.

†† A variational but not self-consistent calculation is available in ref. [32]).

would give the *l*-dependence of the potential. In both cases our model could be used with only minor adjustments. However on the basis of our results it seems that the major challenge is now to find a microscopic explanation of the absorption process.

We would like to acknowledge fruitful discussions with P. H. Heenen and A. Raynal. One of us (J.C.) is very grateful to the members of the Division de Physique Théorique at Orsay for the kind hospitality extended to him.

References

1) D. A. Bromley, J. A. Kuehner and E. Almquist, Phys. Rev. Lett. **4** (1960) 365
2) W. Reilly, R. Wieland, A. Gobbi, M. W. Suchs, J. Maher, R. H. Siemssen, D. Mingay and D. A. Bromley, Nuovo Cim. **13A** (1973) 913
3) R. G. Stokstad *et al.*, ORNL/TM 5935 (1977)
4) H. Feshbach, Proc. Caen Conf., J. de Phys. Suppl. **C5** (1976) 177
5) R. Wieland, A. Gobbi, L. Chua, M. W. Sachs, D. Shapira, R. Stocks and D. A. Bromley, Phys. Rev. **C8** (1973) 37
6) H. Emling, R. Nowotny, D. Pelte and G. Schrieder, Nucl. Phys. **A211** (1973) 600
7) T. M. Cormier, J. Applegate, G. M. Berkowitz, P. Braun-Munzinger, P. M. Cormier, J. W. Harris, C. M. Jachcinski, L. L. Lee Jr., J. Barrette and H. E. Wegener, Phys. Rev. Lett. **38** (1977) 940
8) T. M. Cormier, Proc. XVI Int. Winter Meeting on nuclear physics, Bormio (1978), p. 121
9) P. Sperr, T. H. Braid, Y. Eisen, D. G. Kovar, F. W. Prosser, J. P. Schiffer, S. L. Tabor and S. Vigdor, Phys. Rev. Lett. **37** (1976) 321
10) G. Michaud and E. Vogt, Phys. Rev. **C5** (1972) 350
11) L. Rickertsen, Ph.D. thesis, Yale (1972), unpublished
12) B. Imanishi, Nucl. Phys. **A125** (1969) 33
13) Y. Kando, T. Matsuse and Y. Abe, Proc. 2nd Int. Conf. on clustering phenomena in nuclei, Maryland (1975), p. 532
14) Y. Abe, Y. Dando and T. Matsuse, Prog. Theor. Phys. **59** (1978) 1393
15) H. J. Fink, W. Scheid and W. Greiner, Nucl. Phys. **A188** (1972) 259
16) J. A. Park, W. Greiner, W. Scheid, Phys. Rev. **C16** (1977) 2276
17) O. Tanimura, preprint Tokyo University, INS Rep. **313** (1978)
18) J. Cugnon and R. da Silveira, European Conf. on nuclear physics with heavy ions, Caen (1976), communication p. 59
19) H. Flocard, in Nuclear self-consistent fields, ed. G. Ripka and M. Porneuf (North-Holland, Amsterdam, 1975) p. 219
20) M. Beiner *et al.*, Nucl. Phys. **A238** (1975) 29
21) J. Cugnon, H. Doubre, H. Flocard, M. S. Weiss, to be published
22) M. Baranger and M. Véneroni, Ann. of Phys. **114** (1978) 123
23) H. Flocard, P. H. Heenen and D. Vautherin, to be published
24) N. Cindro and F. Coçu, Proc. Bled Conf., Fizika **9**, suppl 3 (1977) 281
25) P. G. Zint and U. Mosel, Phys. Rev. **C14** (1976) 1488
26) R. E. Peierls and J. Yoccoz, Proc. Phys. Soc. **70** (1957) 381
27) M. Abramowitz and I. A. Stegun, Handbook of mathematical functions (Dover, NY) p. 894
28) M. J. Giannoni, F. Moreau, P. Quentin, D. Vautherin, M. Véneroni and D. M. Brink, Phys. Lett. **65B** (1976) 305
P. Quentin, in 4ème Session d'étude biennale de physique nucléaire, La Toussuire (1975) **C11**
28) W. Nörenberg and H. A. Weidenmüller, Introduction to the theory of heavy-ion collisions, Lectures notes in physics 51 (Springer,Verlag, Berlin, 1976) p. 169
30) M. R. C. McDowell and J. P. Coleman, Introduction to the theory of ion-atom collisions (North-Holland, Amsterdam, 1970) ch. 1
31) A. de-Shalit and H. Feshbach, Theoretical nuclear physics (Wiley, New York, 1974) ch. 6

32) H. Chandra and U. Mosel, Nucl. Phys. **A298** (1978) 151
33) D. M. Brink and G. R. Satchler, Angular momentum (Clarendon Press, Oxford, 1968)
34) M. E. Rose, Multipole fields (Wiley, New York, 1955)
35) F. Shapira, R. G. Stockstadt and D. A. Bromley, Phys. Rev. **C10** (1974) 1063
36) A. Sevgen, Nucl. Phys. **A195** (1972) 415; **A216** (1973) 429
37) G. R. Satchler, Phys. Lett. **39B** (1972) 495; Z. Phys. **260** (1973) 209
38) J. F. Berger and D. Gogny, to be published